Monte Carlo simulation of microstructural transitions in surfactant systems

R. G. Larson

Citation: J. Chem. Phys. **96**, 7904 (1992); doi: 10.1063/1.462343
View online: http://dx.doi.org/10.1063/1.462343
View Table of Contents: http://jcp.aip.org/resource/1/JCPSA6/v96/i11
Published by the American Institute of Physics.

Monte Carlo simulation of microstructural transitions in surfactant systems

R. G. Larson
AT&T Bell Laboratories, Murray Hill, New Jersey 07974

(Received 3 July 1991; accepted 20 February 1992)

In a lattice model of mixtures of idealized surfactant, oil, and water molecules, the microseparation of hydrophobic components (oil and surfactant tails) from hydrophilic ones (water and surfactant heads) is simulated by a Monte Carlo technique. In water, symmetric surfactants, i.e., with heads as long as the tails, achieve lamellar or hexagonal-cylindrical order as the temperature is reduced; the lamellae and cylinders form at surfactant concentrations that are similar to the concentrations at which symmetric block copolymers mixed with homopolymers have been found to form these structures. The lamellae containing tails can have many holes; as the temperature is reduced the holes attain hexagonal order within each layer. At low concentrations in water, symmetric surfactants form spherical micelles; the size distribution of these is computed, as well as the critical micelle concentration. When the surfactant tail is larger than the head, the micelles are cigar shaped or cylindrical. Cylindrical micelles can intersect each other to form a bicontinuous phase. Other disordered bicontinuous phases, including a symmetric spongelike phase, are observed, and the validity of film theories for these phases is examined.

I. INTRODUCTION

In microstructured fluids containing amphiphiles, such as surfactants or block copolymers,[1-3] as one changes a compositional variable, such as the concentration of surfactant, or the ratio of block lengths in a block copolymer, there is typically a progression from body-centered packings of spherical aggregates[4-5] to hexagonally ordered cylinders to ordered bicontinuous structures[6-15] to lamellae. At high temperatures or high concentrations of both oil and water, disordered bicontinuous phases[16-19] also exist. Although these are nearly universal features of amphiphilic mixtures, the detailed microstructures that form, and the conditions under which transitions occur among them, are so complex and system dependent that no single theoretical approach is capable of even qualitatively describing such mixtures over wide ranges of composition and temperature.

For example, although the ordered bicontinuous phases typically occur at compositions between those producing lamellae and those producing cylinders, the type of bicontinuous phase that appears is highly system dependent. In particular, bicontinuous cubic phases seem to occur for nonionic surfactants,[7] for ionic surfactants with two hydrocarbon tails,[20,21] and for short single-tailed ionic surfactants,[7] while "birefringent intermediate phases," including one which is thought to be tetragonal, occur for long-chain ionic surfactants.[7] At least one ionic surfactant, sodium dodecyl sulphate, exhibits transitions to a cubic phase, a tetragonal phase, a rhomboedral phase, and a two-dimensional monoclinic (or deformed hexagonal) phase, as the composition is varied over a narrow range.[6] At least three different types of cubic phases have been observed, having space-group symmetries $Pn3m$, $Im3m$, and $Ia3d$. The surfactant in these cubic phases is thought to be centered on a double-diamond lattice for the $Pn3m$ phase, on a Schwarz' P surface for $Im3m$, and on a gyroid surface for $Ia3d$.[15] The double-diamond and gyroid phases seem to be the most common of the cubic phases. Interestingly, in diblock copolymers, only the double-diamond phase has been identified so far; it is seen in the styrene-diene system.[22] However, other intermediate phases have been observed by Bates and co-workers[14] in poly(ethylenepropylene)-poly(ethylethylene) polymers. The factors controlling the pattern selection among the possible ordered bicontinuous phases appear to be subtle and are as yet not well understood.[20]

In what follows, we hope to show that direct molecular simulation might provide some understanding of the pattern selection process, including the selection among possible ordered bicontinuous phases. First, however, we shall briefly review the strengths and limitations of other theoretical models of surfactant fluid microstructure.

For dilute amphiphilic solutions, in particular, significant theoretical progress has been made using film models. Film models assume that the surfactant lies entirely within thin layers separating oil and water continua. In the earliest such model, Talmon and Prager[23] derived a mean-field free energy containing the entropy of mixing of oil and water domains, and a penalty for bending of the surfactant films separating those domains. Later workers have improved this early model, by describing more realistically the bending energy,[24] by including a microscopic (or molecular) cutoff length scale,[25] and by including the effects of film persistence length,[24,26] film compressibility[25] or incompressibility,[26] and steric-entropic repulsion between films.[27] Film models have yielded useful qualitative and semiquantitative descriptions of the phase behavior of both surfactant,[25-30] and block copolymer phases,[31,32] as well as a description of the L_3 phase,[33] equilibrium vesicles,[34,35] and fluctuation effects.[36] Although in film models molecular details can be expressed only through continuum variables such as interfacial tensions and film bending constants, substantial progress has been made towards predicting those constants from

 0021-9606/92/117904-15$06.00

molecular packing considerations.[37]

Nevertheless, in such models the surfactant layer is collapsed to a two-dimensional film; important details are thereby lost, and film models are most accurate at low amphiphilic volume fractions. Moreover, at least so far, fluctuations have been ignored or included in a perturbative sense only. In addition, in film models a description of each microstructure of interest must be proposed *a priori*, and then its free energy analyzed to determine if it is lower than other candidates. If the microstructure of lowest free energy is not one of the candidates chosen, the true equilibrium microstructure will be missed. In addition, the range of conditions under which film models can be trusted has not yet been clearly established, which is an issue we shall come back to later.

For long polymeric amphiphiles, simplifying statistical approximations are possible that take advantage of the many orientable links of long polymer molecules.[38–40] Thus mean-field or weak-fluctuation theories can be developed; and these have provided a useful starting point for understanding phase transitions and morphology in block copolymer systems at concentrations and temperatures where film models fail. However, these theories do not seem to be extendible to short molecule amphiphiles and, as in film models, the microstructure of lowest free energy will be overlooked if it is not one of the candidates considered.[41]

Molecular simulations in continuous three-dimensional space of amphiphilic aggregates (i.e., micelles), composed of *realistically interacting* amphiphiles, are now feasible and are useful for studying structure and fast fluctuations of these aggregates.[42–45] With such simulations, molecular-scale fluctuations can be studied in detail, even when those fluctuations are large. However, the time scales accessible on the existing and foreseeable computers make these techniques untenable for the study of problems involving large distances or long-time scales, as is required in the determination of the equilibrium structure of a microemulsion phase.

This limitation of molecular-scale modeling has been avoided by Widom[46] and by Schick and co-workers[47] who analyzed highly simplified "Ising-type" lattice models in which the molecules occupy only one or two sites. Qualitative features of the phase behavior and structure of real surfactant systems at large distance scales can be captured by these models. But in these models virtually all distinctive molecular details are effaced, rendering the models incapable of capturing in any detail the effects of surfactant architecture, except those that can be included empirically in the interaction parameters.

Thus, because of the complexity and richness of surfactant-containing fluids, several different theoretical approaches have proved fruitful, but none are without serious drawbacks. In particular, none of the aforementioned models is likely to be able to address the question of how molecular structure influences the competition among ordered phases, including ordered bicontinuous phases, at high surfactant concentration.

In this paper, we pursue further a "Flory-type" lattice model introduced earlier[48,49] for the simulation of self-assembled surfactant microstructure, in which the surfactant molecules occupy a sequence of several lattice sites. Thus this model lies between the Ising-type lattice models of Widom and Schick *et al.*, and more realistic off-lattice simulations. Compared to the simple lattice models, this Flory-type model is less affected by lattice artifacts and, because of the more realistic description of the surfactant molecule, is capable of better describing both surfactant microstructures and the effect of surfactant properties—such as head and tail lengths—on those microstructures. Thus, we believe that the Flory-type model is the simplest model that is likely to be capable of analyzing qualitatively the influence of molecular properties on pattern selection, particularly among ordered bicontinuous patterns. Our Flory-type lattice model has only simple nearest-neighbor interactions and is, in this respect, similar to most models of polymer systems, but the molecules are small, like surfactant molecules. Thus, the properties of the model also make it useful as a means of understanding and bridging the differences between polymeric and small-molecule amphiphiles. Although Flory-type models require much more computation than do the simpler Ising-type lattice models, the speed of computers available now and in the near future will, we believe, make the use of the former especially fruitful in the study of equilibrium microstructures of surfactant-containing fluids.

II. OVERVIEW OF THE FLORY-TYPE LATTICE MODEL

In our Flory-type lattice model, the surfactant molecules are confined to a cubic lattice and interact only with nearest and diagonally nearest neighbors; the usual periodic boundary conditions are employed. Oil and water molecules occupy single sites on the lattice, and each amphiphile occupies a sequence of adjacent or diagonally adjacent sites. The amphiphile sites can be occupied by either head (water-loving) or tail (oil-loving) units. The interaction energy is taken to be pairwise additive. For simplicity in this version of the model, we let the interaction energy of a head unit with a neighbor, say an oil, be the same as the interaction energy of a water unit with oil. Similarly the interaction energy of a tail unit with a neighbor is assumed to be the same as that of an oil unit with that same neighbor; thus head and tail units are chemically identical to water units and oil units, respectively. With this choice for the interaction energies, the system can be characterized by a single dimensionless interaction energy parameter w, which is the interaction energy per oil/water contact, divided by $k_B T$. The nomenclature $H_i T_j$ defines a surfactant that consists of a string of i head units attached to j tail units.

Rearrangements of the molecules in the system take place by oil/water interchanges, and by kink and reptation motions of the amphiphile.[48] Each attempt at one of these movements shall hereafter be called a Monte Carlo (MC) step. To prepare equilibrium or near-equilibrium states, we disperse the molecules on the lattice in some near-random fashion, set the temperature to infinity (i.e., $w = 0$), and let the system equilibrate by the moves listed earlier. We then cool the system by increasing w in small increments, allowing many millions of MC steps between each increment, so that thermal equilibrium is maintained. At high tempera-

tures $1/w$, thermal equilibrium is attained rapidly, in a few million MC steps, but at low temperatures, i.e., $w \geqslant 0.10$, thermal equilibration can require billions of MC steps on the largest lattices considered here ($40\times40\times40$).

At each temperature, we monitor the average energy per lattice site; at the lower temperatures on large lattices this average is taken over a billion or so MC steps. When the averaged energy appears to reach a steady state—that is, when it varies by less than about 0.2% over a couple of billion attempted moves (on $40\times40\times40$ lattices, fewer than this on smaller lattices)—we assume that the system has equilibrated at that temperature and then we increase w by another small increment. Experimentation with different rates of cooling has given us confidence that our cooling regimen keeps us close to equilibrium,[49] except near first-order thermodynamic transitions. As discussed later, near such transitions we often see hysteresis when a system that has been cooled through a transition is reheated. Details of the typical cooling regimens can be found in Ref. 49, and in the figure captions of this paper.

Although this Flory-type model has made possible the simulated self-assembly of lamellar, cylindrical, and spherical morphologies, as well as bicontinuous structures, at this stage of its development it lacks the complicating details of real systems, such as hydrogen bonding, electrostatic interactions, and detailed molecular-shape effects. While its featurelessness seriously limits it as a model of any specific experimental system, it could serve as an ideal model system for studying and testing theories and ideas of amphiphilic pattern formation. Seen in this light, the most serious potential drawback of the present version of the model is that it is realized on a cubic lattice. Fortunately, however, we have been able to show[49,50] that the directional bias one expects on a cubic lattice is weak for our simulations; this bias is apparently suppressed because we have made the interaction energies between all twenty six nearest and diagonally nearest neighbors equivalent to each other, and have allowed the surfactant chain to be connected along both nearest and diagonally nearest-neighbor sites. In particular, we have found that patterns in which there is at least one infinite wavelength (i.e., lamellar or hexagonal patterns) orient so that the characteristic spacings of the pattern (e.g., the interlamellar spacing of a lamellar pattern) are commensurate with the lattice dimensions. In these cases, when the lattice size is changed, the pattern reorients so that nearly the same characteristic spacings are retained on a different-size lattice. When there is no infinite wavelength, however, as for example on a pattern with cubic symmetry, reorientation of the pattern will not help it fit on a finite lattice, and the size of the lattice affects the pattern that is chosen.[50]

III. RESULTS

In this communication, we focus on the microstructural transitions that occur when one changes temperature, concentration, or the length of the surfactant head or tail. We wish to show that the model gives results consistent with experiment and with other theoretical techniques, that it can provide a useful new bridge between polymeric amphiphiles and surfactants, and, most importantly, that it can make predictions about pattern transitions that are difficult or impossible to obtain by other theoretical approaches.

Broadly speaking, in amphiphilic systems, microseparation, ordering, geometric, and topological transitions can occur, often in combination. To illustrate the distinctions among these, consider a solution of surfactant in water at high temperature where the surfactant is randomly dispersed. As the solution is cooled, a continuous (though possibly fairly sharp) transition occurs to a disordered arrangement of spherical micelles. This is a *microseparation* transition, since it involves the separation of tail units from their hydrophilic environment into the hydrophobic cores of spherical micelles. On further cooling, the micelles might undergo a continuous *geometric* transition to long rodlike or wormlike micelles, or a discontinuous *ordering* transition to a bcc packing of spherical micelles. If wormlike micelles form and their concentration is increased, they can intersect each other and undergo a *topological* transition to a bicontinuous phase.

We divide our results into two sections. In the first, we consider systems that undergo an ordering transition when cooled. We find that as systems composed of the surfactants H_3T_3 and H_4T_4 in oil and water with an oil/water ratio of unity are cooled, an ordering transition occurs to a lamellar phase. Even at temperatures above the ordering transition, there is significant microseparation of hydrophobic and hydrophilic components because the correlation length of composition fluctuations is greater than the size of a lattice cell. When the surfactant volume fraction C_A is high (0.60), the ordering transition is a sharp one. When C_A is low (0.20), the transition is gradual, and occurs in the following way: As the temperature is lowered, the surfactant molecules straighten out, and collect into a wrinkled skin that separates a continuous oil domain from a continuous water domain. With a further decrease in temperature, the surfactant molecules straighten out further, the skin flattens, and the oil and water continua order into lamellae with holes. With still further cooling, the holes disappear and the skin divides into parallel sheets that separate alternating lamellae of oil and water.

When various concentrations of H_3T_3 or H_4T_4 in water only are cooled, we again find ordering transitions; at a high concentration ($C_A = 0.8$), the ordered pattern is lamellar, and at lower concentrations ($C_A = 0.45$–0.65), it is a hexagonal array of cylinders. At an intermediate surfactant concentration ($C_A = 0.75$) two transitions occur: the first to lamellae densely populated with holes in the layers containing tails; and in the second the holes attain a hexagonal order in each layer. For a concentration slightly below the minimum required for a cylindrical hexagonal phase ($C_A \approx 0.45$), there is on cooling a continuous transition to a mixture of disordered spherical and wormlike micelles. At still lower concentrations ($C_A = 0.35$), cooling produces a continuous transition to disordered spherical micelles.

In the second section of results, we consider the changes in micellar shape that occur as the lengths of the surfactant heads and tails are varied at low surfactant concentrations ($C_A \leqslant 0.20$). We find that while symmetric surfactants H_3T_3

and H_4T_4 form spherical micelles at inverse dimensionless temperatures greater than or equal to $w = 0.1538$, surfactants in which the tail is significantly longer than the head, such as H_2T_6, form cylindrical micelles. Even at rather low surfactant concentration, these intersect each other to form a bicontinuous phase. In an intermediate case in which the tail is only slightly longer than the head, namely H_3T_4, spherical micelles are initially formed as the system is cooled; eventually, at a lower temperature of $w = 0.1538$, some of these agglomerate, forming a bimodal mixture of spherical and cigar-shaped micelles. Having thus summarized our results, let us now present them in detail, starting with the completely symmetric systems, i.e., solutions containing H_3T_3 or H_4T_4 at an oil/water ratio of unity.

A. Microseparation and ordering transitions

1. For an oil/water ratio of unity

Figure 1 shows slices of the $40\times40\times40$ system containing 60% by volume H_4T_4, with 20% oil and 20% water, at $w = 0.1120$ (upper) and at $w = 0.1130$ (lower). These correspond, respectively, to an isotropic disordered state and an ordered *smectic lamellar* state that is attained when the disordered state is cooled. The tail units are shown as circles and the oil units as asterisks; the water and head units are not shown. Figure 2 plots the ensemble average of the dimensionless energy per lattice site, $\langle E \rangle$, as a function of w during cooling and subsequent reheating of this H_4T_4 system and of the same concentration of H_3T_3 on $20\times20\times20$ and $40\times40\times40$ lattices. The value of $\langle E \rangle$ at each w was obtained by averaging over at least 4×10^7 MC steps on the $20\times20\times20$ lattice, and 4×10^8 MC steps on the $40\times40\times40$ lattice. There is a distinct drop in average energy when the 60% H_4T_4 and H_3T_3 systems order. For H_4T_4, ordering occurs at $w = 0.1130$ on the $40\times40\times40$ lattice and at $w = 0.1120$ on the $20\times20\times20$ lattice. Note that apart from this small difference in ordering temperatures, there is little difference between the two lattices in the relationship between $\langle E \rangle$ and w. On reheating the $40\times40\times40$ H_4T_4 system, a jump occurs at $w = 0.1080$, and inspection of cross sections shows that the system disorders at this temperature. This hysteresis in the transition temperature is characteristic of first-order phase transitions. On a smaller $20\times20\times20$ lattice, the hysteresis in the transition is negligible—Fig. 2 also shows that for the $20\times20\times20$ lattice, $\langle E \rangle$ vs w on reheating is almost the same as that obtained on cooling. Thus on reheating, the ordered state is more unstable on the smaller lattice than it is on the larger lattice, evidently because a fluctuation of given size affects a larger fraction of the whole system on a small lattice than it does on a big lattice. Similar behavior is found for 60% H_3T_3 in equal amounts of oil and water.

Figures 3–5 show the lamellar ordering transition on a $40\times40\times40$ lattice for 20% H_4T_4 in 40% each of water and oil. Figure 3 shows a slice of this system at $w = 0.1077$ (upper) and after cooling to $w = 0.1231$ (lower). In Fig. 4, *two mutually perpendicular slices* of a single system are shown after cooling to $w = 0.1385$. Thus Fig. 4 shows two faces of a cube of material. Figure 5 shows two mutually perpendicular slices of the system after it has been further cooled to $w = 0.1424$. The transition in Figs. 3–5 is much more nearly continuous than the ordering transition for 60% H_4T_4 depicted in Fig. 1. In fact, Figs. 3–5 suggest that smectic lamellar order is probably achieved in two stages. In the first stage, a disordered bicontinuous "sponge" phase (Fig. 3, lower panel) achieves lamellar order (Fig. 4), but the lamellae are interrupted by holes. In the second stage, the holes disappear (see Fig. 5). Consistent with the gradualness of the ordering transition for 20% H_4T_4, Fig. 2 shows that the any jump in average energy $\langle E \rangle$ at either stage of the transition is so

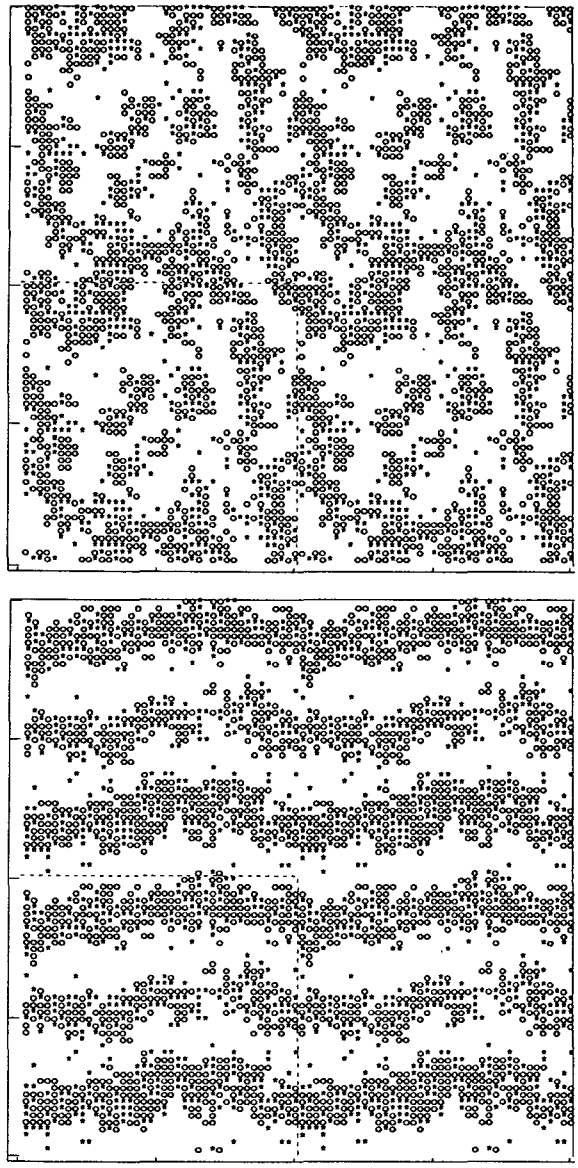

FIG. 1. Cross-sectional slices of $40\times40\times40$ lattice containing 60% H_4T_4 and equal parts of oil and water. The structure at the top was obtained after slowly cooling a random system in small temperature steps to $w = 0.1120$. It was then subjected to a small step decrease in temperature to $w = 0.1130$; after $T = 3.2\times10^9$ MC steps, the structure on the bottom appeared. In this and following figures, the images were obtained by periodic replication of the simulated volume, which here is enclosed in dashed lines. The circles represent tail units; the asterisks are oil units.

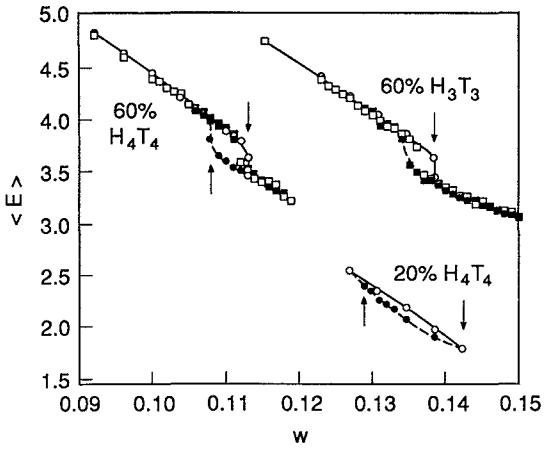

FIG. 2. Average dimensionless ensemble energy per unit lattice site $\langle E \rangle$ as a function of dimensionless inverse temperature w for H_4T_4 and H_3T_3; $\langle E \rangle$ is the average number of contacts between hydrophobic units (tail and oil units) and hydrophilic units (head and water units) per lattice site, excluding the unbreakable contacts that connect each head to the tail of the amphiphile. The open symbols are for cooling and the closed symbols for reheating; the circles are for the $40\times40\times40$ lattice and the squares for the $20\times20\times20$ lattice. The arrows mark the transition temperatures on $40\times40\times40$ lattices. The down arrow marks the ordering transition on cooling; the up arrow marks the disordering transition on reheating.

small that it is imperceptible; it is much smaller than for 60% H_4T_4. Despite the smallness of the energy difference between ordered and disordered solutions containing 20% surfactant, there is a large hysteretic difference between the ordering and disordering temperatures. We are here taking the "ordering temperature" to be the temperature at which the surfactant films become simply connected, so that the water and oil layers are without holes. The disordering transition is conversely taken as the temperature at which the surfactant film becomes multiply connected.

The average energy $\langle E \rangle$ just above the ordering transition to the smectic lamellar phase is much smaller for the solution containing 20% surfactant than it is for the 60% solution. This means that microseparation is much more complete at the ordering transition for 20% H_4T_4 than for 60% H_4T_4. This result is not surprising, since the amount of oil and water available to participate in the microseparation is much greater for the 20% system than for the 60% system and oil and water with no surfactant would macroseparate at $w\approx0.09$. Thus, in the 20% H_4T_4 system, the oil and water are already highly segregated at a temperature somewhat above that required for ordering. The surfactant (represented by circles in Fig. 3) at this temperature forms a "skin" on the interface between the oil and water regions, as can be seen in Fig. 3 (lower panel). As the temperature is lowered, this "skin" becomes smoother and less distorted by thermal fluctuations. Eventually, the skin develops a preferred orientation, albeit with holes (see Fig. 4). At still lower temperature, the holes disappear, and the system develops unambiguous smectic order (see Fig. 5). The ordering transition in the 20% H_4T_4 system may be a good candidate for modeling by the film theories referred to in the Introduction. In-

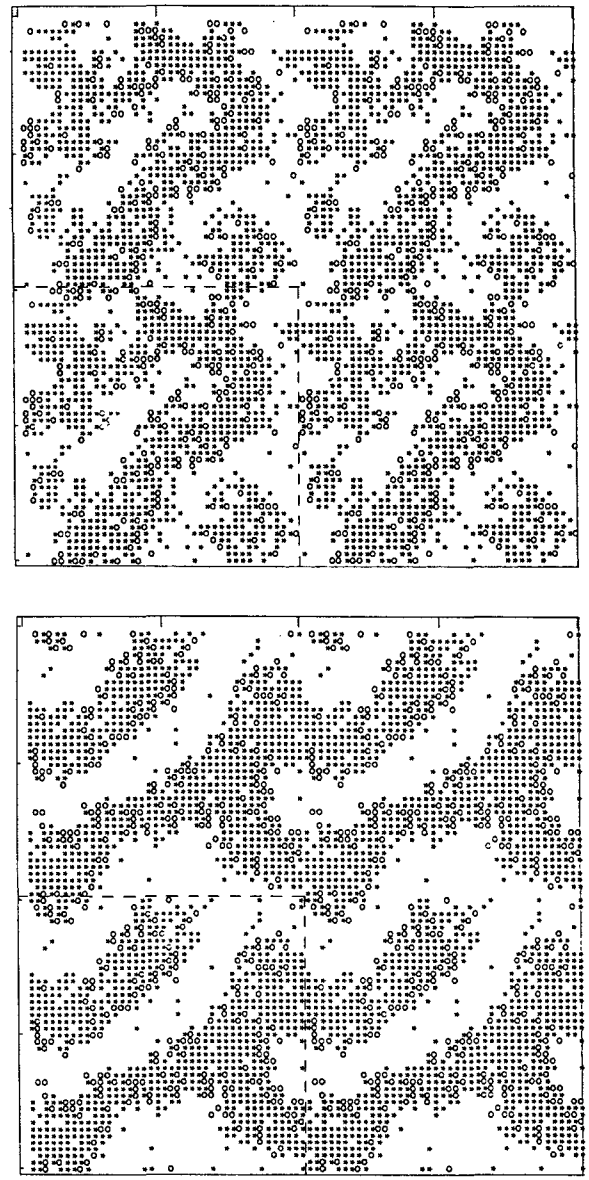

FIG. 3. Slices from a $40\times40\times40$ lattice containing 20% H_4T_4 and equal parts of oil and water at two relatively high temperatures. The image on the top was obtained at $w=0.1077$; the image at the bottom was obtained from the one on the top $T=8\times10^8$ MC steps after changing w from 0.1077 to 0.1231. These images contain periodic replications, as described in the caption to Fig. 1.

deed, in a film theory by Huse and Leibler,[29] it is speculated that the transition from an isotropic disordered phase to a smectic lamellar phase might occur in two steps by way of an intermediate *nematic lamellar* phase, in which the films have preferred orientational order but no long range positional order. It is possible that the structure shown in Fig. 4 might represent a small piece of such a nematic lamellar phase. However, more thorough study of this structure on a larger lattice will be required before this can be asserted.

For 60% and 20% H_3T_3 in equal parts of oil and water, we obtain ordering transitions similar to those for H_4T_4, except that the temperatures at which the transitions occur

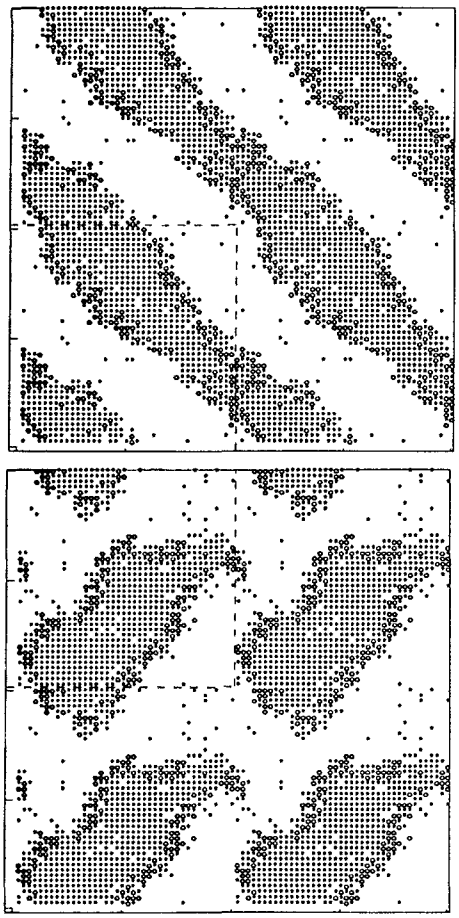

FIG. 4. Two mutually perpendicular slices from the structure formed by cooling to $w = 0.1385$ the system depicted in Fig. 3; the cooling occurred in small steps in w of $\Delta w = 0.0038$, with at least 8×10^8 MC steps between each temperature step.

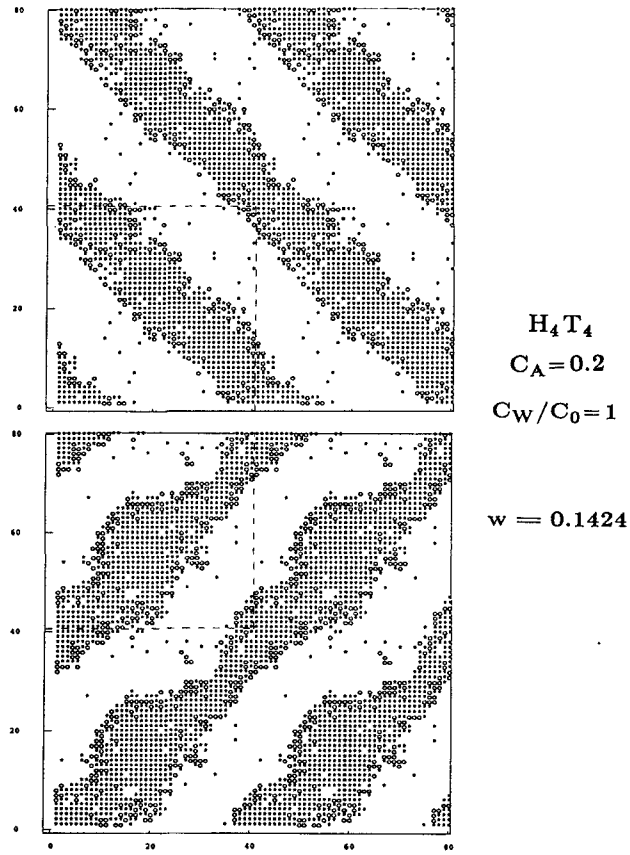

FIG. 5. The system depicted in Fig. 4 after step cooling to $w = 0.1424$ and equilibrating for 1.6×10^9 MC steps.

are lower for H_3T_3 than for H_4T_4 (see Fig. 2). As with H_4T_4, the ordering transition for 60% surfactant is sharp, and for 20% surfactant the lamellae appear first with holes in them that disappear on further cooling. The inverse dimensionless transition temperatures w_c at which ordered lamellae without holes form on cooling, are given in Table I. Also given are the values of zNw_c, where N is the number of sites occupied by the surfactant (six for H_3T_3 and eight for H_4T_4) and $z = 26$ is the coordination number. According to the mean-field Leibler theory[39] for symmetric diblock copolymers with no solvent, $zNw_c = 10.5$. Fredrickson and Helfand[40] showed that fluctuations cause an increase in zNw_c, yielding $zNw_c = 10.5 + 41N^{-1/3}$. Although the Fredrickson–Helfand theory is perturbative—becoming strictly valid only as $N\rightarrow\infty$—and thus certainly cannot be applied to our small-molecule system in any detail, it does suggest that zNw_c should be much larger than 10.5 for our system, that the transition from disorder to an ordered state should be a strong one, i.e., it should involve a large jump in the compositional order parameter, and that fluctuation effects should be very important. All these implications of the Fredrickson–Helfand theory hold for our systems with high surfactant concentration.

While the Fredrickson–Helfand theory, if pressed, might tell us something about the role of fluctuations near the ordering transition for amphiphiles with little or no solvent, film models tell us that for systems that are rich in solvent and dilute in surfactant, an ordering transition from a disordered bicontinuous phase (such as in Fig. 3) to a smectic lamellar phase (such as in Fig. 5) occurs when the temperature is lowered enough that the surfactant-laden interfacial film separating oil and water becomes stiff enough. One expects the transition to occur when the persistence length of the film becomes comparable to or greater than the oil or water domain size of the disordered bicontinuous structure. This prediction seems to be qualitatively consis-

TABLE I. Inverse ordering temperatures w_c.

Surfactant	Concentration	w_c	zNw_c
H_2T_2	80%	0.2154	22.4
H_3T_3	60%	0.1366	21.3
H_4T_4	60%	0.1120	23.3
H_3T_3	20%	0.1722	26.9
H_4T_4	20%	0.1405	29.2

tent with what one observes in Figs. 3–5. Since the film model assumes that the surfactant resides entirely on a skin with a nearly constant area of occupation per surfactant molecule, the model also predicts that the lamellar spacing d should be inversely proportional to surfactant concentration. Table II presents the lamellar spacings d for H_4T_4 in equal amounts each of oil and water, for lattices large enough that finite lattice size effects are expected to be less than about 10%.[51] The last column of Table II shows that the product $C_A d$ depends on C_A when $C_A \geqslant 0.5$, but may be approaching a constant as C_A is reduced.

Andelman *et al.*,[26] have predicted, using a film model, that the ordering temperature should *decrease* with decreasing surfactant concentration, because of a renormalization-induced reduction in the effective bending constant at low surfactant concentration. Thus at a fixed temperature, and at a fixed oil/water ratio of, say, unity, when the surfactant concentration decreases, there is predicted to be a transition from an ordered lamellar to a disordered bicontinuous phase. This is certainly consistent with our findings; Fig. 2, for example, shows that at an inverse dimensionless temperature of roughly $w = 0.12$, there is a lamellar phase for H_4T_4 when $C_A = 0.6$, and a disordered bicontinuous phase when $C_A = 0.2$. Presumably for $w = 0.12$ there is an intermediate concentration regime for which both lamellar and the disordered bicontinuous phases coexist.

However, some important aspects of the ordering transition in our system are not described by the film models. An important assumption of film models is that the surfactant layer contains no internal degrees of freedom that change significantly over the range of composition and temperature to which the model is applied. This means that the distribution of conformations of the surfactant molecules should be insensitive to composition and temperature. We test this assumption in Fig. 6 by plotting the mean-square end-to-end separation $\langle R^2 \rangle$ of the first and last units on the surfactant chain as a function of w. For $C_A = 0.20$ at an oil/water ratio of unity, $\langle R^2 \rangle$ remains near its high-temperature asymptote $\langle R^2 \rangle \approx 16.6$ until w is increased to about 0.08, which is close to the value of w at which a surfactant-free 50/50 mixture of oil and water would spinodally decompose. Thus the tendency of oil and water to separate from each other at $w \approx 0.08$ evidently leads to stretching of surfactant chains, thereby allowing more complete separation of oil from water, while maintaining a high entropy of mixing of oil with surfactant tails and water with surfactant heads. The degree of stretch of surfactant chains increases with increasing w throughout

TABLE II. Spacings in lamellar phases for H_4T_4.

C_0/C_w	C_A	Symmetry	Lattice	Spacing d	$C_A d$
1	0.80	Lamellar	20×20×20	8.9	7.1
1	0.60	Lamellar	40×40×40	9.4	5.6
1	0.50	Lamellar	20×20×20	11.6	5.8
1	0.30	Lamellar	30×30×30	13.4	4.0
1	0.20	Lamellar	40×40×40	23.1	4.6

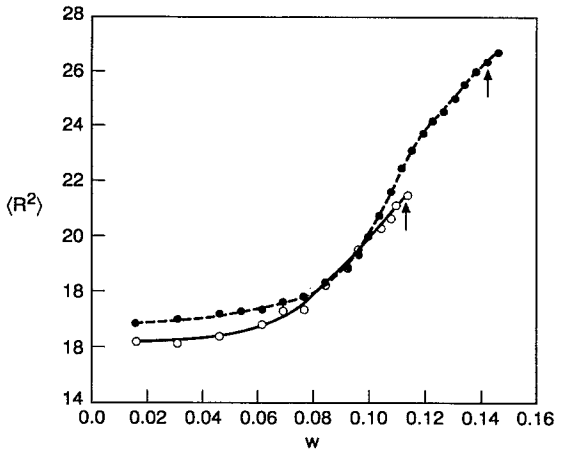

FIG. 6. The mean-square end-to-end separation of amphiphile chain ends as a function of inverse dimensionless temperature w for 20% amphiphile (open symbols) and 60% amphiphile (closed symbols) at an oil/water ratio of unity. The arrows show where the ordering transition occurs.

the range in which the two-step ordering transition occurs to the lamellar phase without holes. As the chains stretch during cooling, one would expect them to pack together more closely, thus reducing the amount of interfacial area. Indeed, it is apparent in Figs. 3–5 that the amount of interfacial area decreases as w increases; further work is needed, however, to quantify this apparent decrease in interfacial area. Since properties of the film, especially bending constants, are likely to be sensitive to changes in the surfactant conformation distribution and in the packing density of chains at the interface, one must question the ability of at least the simplest film models to describe the ordering transition in our model system. We must note, however, that in our model, the oil is monomeric and the surfactant very flexible. Less chain stretching probably occurs for stiffer surfactants that change conformations less readily, and for longer oil molecules that penetrate the surfactant tail layer to a lesser extent.

Figure 6 also plots $\langle R^2 \rangle$ vs w for $C_A = 0.60$ at an oil/water ratio of unity. Chain stretching also occurs in this more concentrated solution; the results in Fig. 6 are similar to those reported for simulations on longer chains by Minchau *et al.*[52] and observed experimentally in diblock copolymers.[53,54] Chain stretching has been accounted for in weak segregation theories of diblock copolymers.[55] The difference in $\langle R^2 \rangle$ between 20% and 60% surfactant solutions at small w is caused by the concentration dependence of the excluded volume effect.

2. With no oil

When H_4T_4 systems containing 45%–65% surfactant mixed with water, but no oil, are cooled, quasihexagonal, i.e., distorted hexagonal, phases form (see Fig. 7). The distortion, which is induced by the finite lattice size, is modest or small for lattices as large or larger than $30 \times 30 \times 30$.[50] As a result of the distortion, the six cylinders closest to a given cylinder are not all the same distance from that cylinder. Instead, one obtains the three characteristic intercylinder spacings listed in Table III. The spacing $\bar{d}$ used in the last

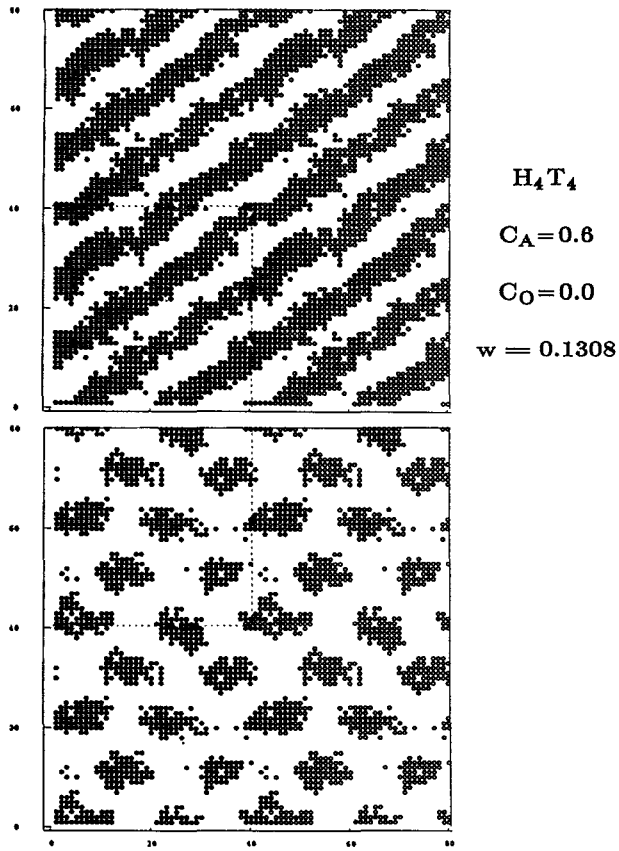

FIG. 7. Two mutually perpendicular slices of a $40\times40\times40$ lattice containing 60% H_4T_4 in water at $w = 0.1308$, obtained 9.6×10^9 MC steps after cooling a system that had been equilibrated at $w = 0.1270$. When reheated in steps Δw of 0.0038, this system disorders at $w = 0.1116$.

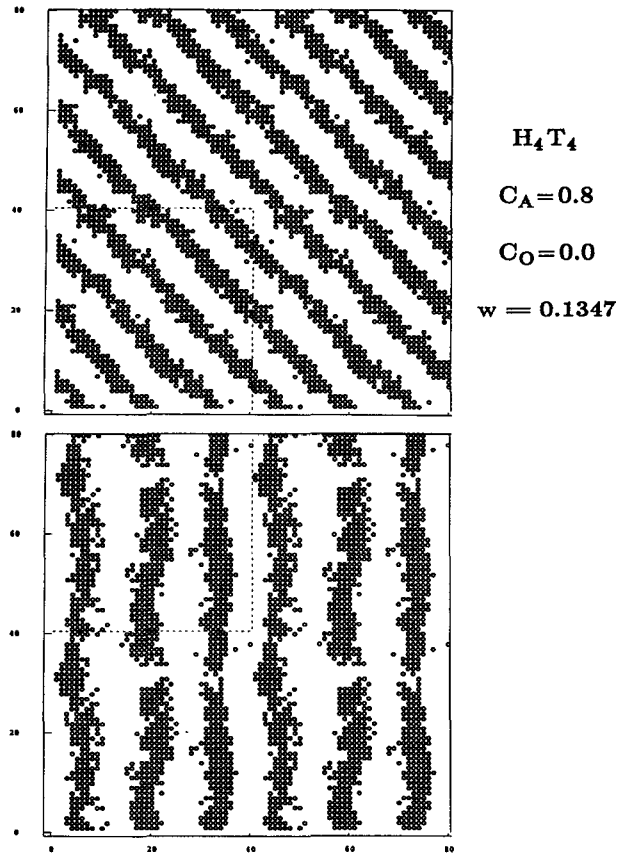

FIG. 8. Two mutually perpendicular slices of $40\times40\times40$ lattice containing 80% H_4T_4 in water at $w = 0.1347$, obtained 9.6×10^9 MC steps after cooling a disordered system that had been equilibrated at $w = 0.1308$.

column of Table III for the quasihexagonal symmetries is the arithmetic average of these three spacings. The concentration C_H is the concentration of hydrophilic units; for symmetric surfactants, $C_H = C_w + \frac{1}{2}C_A$. To a first approximation, we believe that the concentration of hydrophilic units determines which ordered morphology is obtained.

At a higher surfactant concentration, $C_A = 0.80$, we find on cooling an ordering transition at $w = 0.1347$ to lamellae (see Fig. 8). The ordering transitions to lamellar and hexagonal symmetry shown in Figs. 7 and 8 are sharp transitions, like the transitions for 60% H_3T_3 and 60% H_4T_4 with equal amounts of oil and water. Note in Fig. 8 that the lamellae have holes in them. These lamellar holes do not exist at the ordering transition for a system containing a similarly high surfactant concentration but with an oil/water ratio of unity (see Fig. 1). Thus the lamellar holes seen for this surfactant at an oil/water ratio of zero (see Fig. 8) exist because of an oil/water compositional asymmetry. However, lamellar holes also exist in compositionally symmetric systems, such as in Fig. 4; these latter holes apparently occur because

TABLE III. Spacings in lamellar and quasihexagonal phases for H_4T_4.

C_O/C_w	C_A	C_H	Symmetry	Lattice	Spacing d	$\bar{d}$
0	0.45	0.775	Hexagonal	30×30×30	12.3|12.3|12.3	12.3
0	0.50	0.75	Hexagonal	30×30×30	12.3|12.3|12.3	12.3
0	0.55	0.725	Quasihexagonal	30×30×30	10.8|10.8|11.1	11.0
0	0.60	0.70	Quasihexagonal	40×40×40	11.1|11.4|11.4	11.3
0	0.65	0.675	Quasihexagonal	30×30×30	10.8|10.8|11.1	11.0
0	0.70	0.65	Disordered bicontinuous	40×40×40		
0	0.75	0.625	Lamellar with holes	40×40×40	9.4	9.4
0	0.80	0.60	Lamellar with holes	40×40×40	9.4	9.4

of gradualness in the ordering transition at low surfactant concentrations. Thus lamellar holes can exist in at least two different types of systems, and for at least two different reasons. Lamellae with holes similar to these in Fig. 8 have been seen experimentally by microscopy in a system containing a slightly asymmetric low-molecular-weight diblock copolymer of polystyrene and polyisoprene.[51] Such holes may be common in nonpolymeric and low-molecular-weight polymeric amphiphiles.

If the surfactant concentration C_A is lowered modestly, from 0.80 to 0.75, the density of holes is greatly increased (see Fig. 9). Figure 10(a) shows a slice of this system taken parallel to the lamellae and within one of the layers with holes at $w = 0.1500$. The holes are spatially disordered, but as w is increased on the $40\times40\times40$ lattice, the holes order into a slightly distorted hexagonal pattern with hole spacings of 15.0|15.4|15.9; see Fig. 10(b). The holes in the adjacent layers do not lie along a normal to the lamellar layers; nor are they in the simplest possible staggered arrangement. However, as will be discussed elsewhere,[50] patterns with three-dimensional order are particularly susceptible to distortion because of the small size of our lattices. Thus studies using a variety of lattice sizes will be required to determine the three-dimensional order that occurs in this system. It is probable, however, that the true symmetry corresponds to

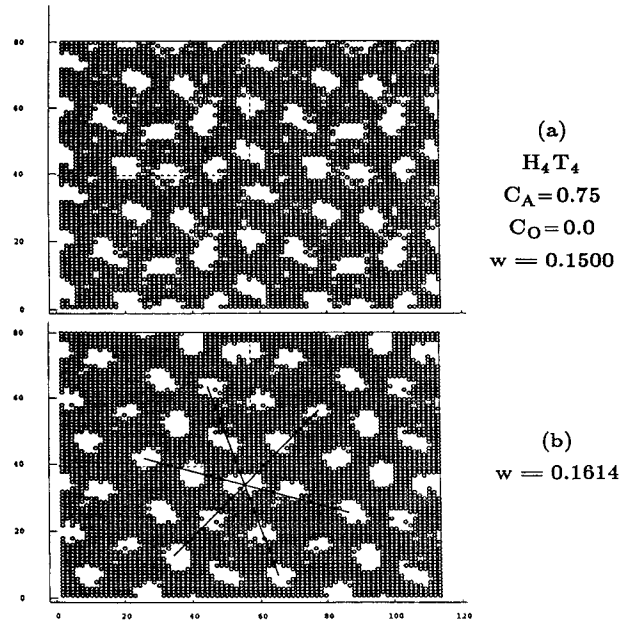

FIG. 10. A diagonal slice of $40\times40\times40$ lattice containing 75% H_4T_4 in water at (a) $w = 0.1500$ and (b) $w = 0.1614$.

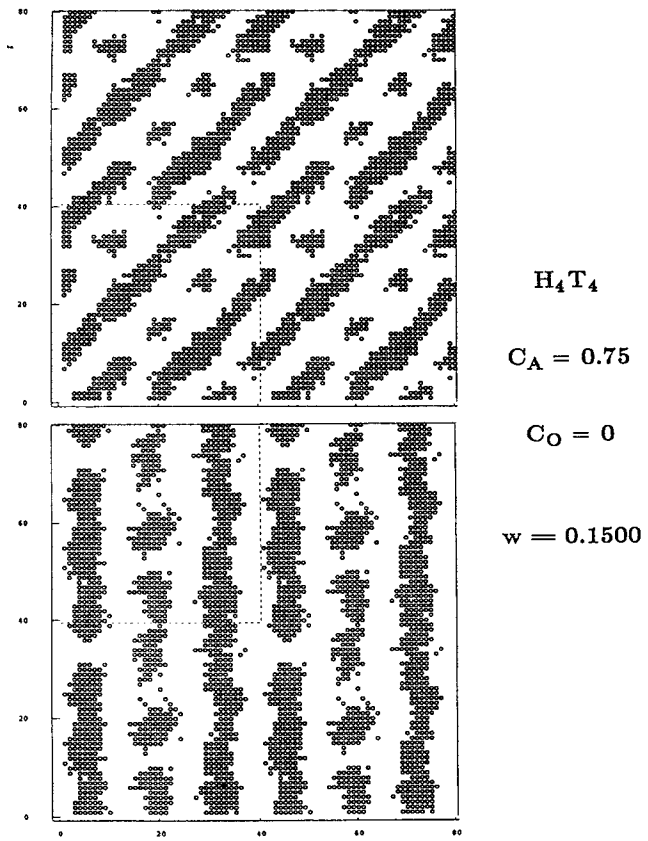

FIG. 9. Two mutually perpendicular slices of $40\times40\times40$ lattice containing 75% H_4T_4 in water at $w = 0.1500$.

one of the noncubic "birefringent intermediate" phases, involving hexagonally ordered holes within each layer. Since the preferred packing of holes is likely to be sensitive to the hole concentration, and the density of holes increases rapidly as C_A is reduced from 0.8 to 0.75, there may be more than one intermediate phase at low temperatures in the concentration range $C_A = 0.70$–0.80. This concentration range will be studied carefully in future work. It will also be interesting to see what intermediate phases form in our model when the surfactant head and tail lengths are varied, when a cosurfactant (a short second amphiphile) is added to the solution, when a second tail is added to the surfactant, or when other interaction parameters are introduced.

The transitions to lamellar and cylindrical morphologies in our simulations are similar to those observed by Winey *et al.*[56,57] when low-molecular-weight homopolymer polystyrene was added to a nearly symmetric polystyrene–polyisoprene diblock copolymer. The diblock in these experiments had a modest molecular weight of 49 000. In one series of experiments the homopolymer molecular weight was 6000, roughly $\frac{1}{8}$ that of the diblock, making this system analogous to the simulations for H_4T_4 in water, in that H_4T_4 occupies 8 times the volume of the water. Of course the experiments of Winey *et al.* differ from the simulations in that even though the homopolymer molecules were rather short, they were still long enough to possess many possible molecular conformations; whereas the solvent in the simulation has only one conformational state. The number of conformations available to a polymer molecule is conveniently indexed by modeling the molecule as a sequence of freely jointed rods; the number and length of the rods are then adjusted to match the molecule's contour length and radius of gyration. For polystyrene, a match is obtained when the

number of rods equals the molecular weight divided by about 1000.[58] Thus, homopolystyrene of molecular weight 6000 should be represented by a freely-jointed chain of some six rods and the diblock by a few dozen rods.

Despite the mismatch between simulation and these experiments in the number of molecular conformational states, we find agreement in the concentrations C_H at which the lamellar, cylindrical, and intermediate morphologies occur; compare Table IV with Table III. In Table IV we define C_H as the total volume fraction of styrene contained in both the diblock and the homopolymer. Not only is there close agreement in the concentration ranges over which hexagonal and lamellar phases exist, but the ratio of the spacing between cylinders to that between lamellae is 1.26 in the experiments with polymers, which is close to that obtained in the simulations.

In Table IV, OBDD stands for "ordered bicontinuous double diamond;" this cubic phase is found in the experiments for a styrene concentration of 65%. In the simulations, bicontinuous structures are also found when $C_H = 0.65$ (see Fig. 11), but these bicontinuous structures are *disordered* at temperatures comparable to or even somewhat lower than those at which lamellar and quasihexagonal patterns form for $C_H = 0.6$ and $C_H = 0.7$, respectively. We expect that as the temperature is lowered further, an ordering transition will occur at $C_H = 0.65$ also; we hope to have more to say about this in an upcoming publication.[50]

We summarize the structures we have obtained so far for H_4T_4 in water on the approximate phase diagram of Fig. 12(a). In Fig. 12(a), the dimensionless transition temperatures are only approximations to the equilibrium values, since the transitions are hysteretic. This rough phase diagram is remarkably similar to the phase diagram for lithium perfluorooctanoate in water determined by Kekicheff and Tiddy[7] [see Fig. 12(b)] in that the ordered phases in Fig. 12(a) are the same or similar to those in Fig. 12(b), as are the ranges of compositions over which the ordered phases occur. Note also that in both diagrams there is a window of compositions between hexagonal and lamellar phases in which there is a disordered phase; but in the simulations the disordered phase seems to persist to comparatively lower temperatures than is the case in the experimental system. Perhaps in this window the run times required to obtain the ordering transition are especially long, and long runs would then be required to obtain equilibrium for compositions within this window. We note that on small $17\times17\times17$ or $20\times20\times20$ lattices compositions within this window do or-

TABLE IV. Morphologies and spacings for 6000 MW polystyrene in polystyrene–polyisoprene diblock (from Ref. 57).

C_H, Styrene volume fraction	Morphology	Spacing (nm)
0.75	Hexagonal	49.8
0.70	Hexagonal	49.6
0.65	OBDD	58.4
0.60	Lamellar	39.7
0.55	Lamellar	38.9

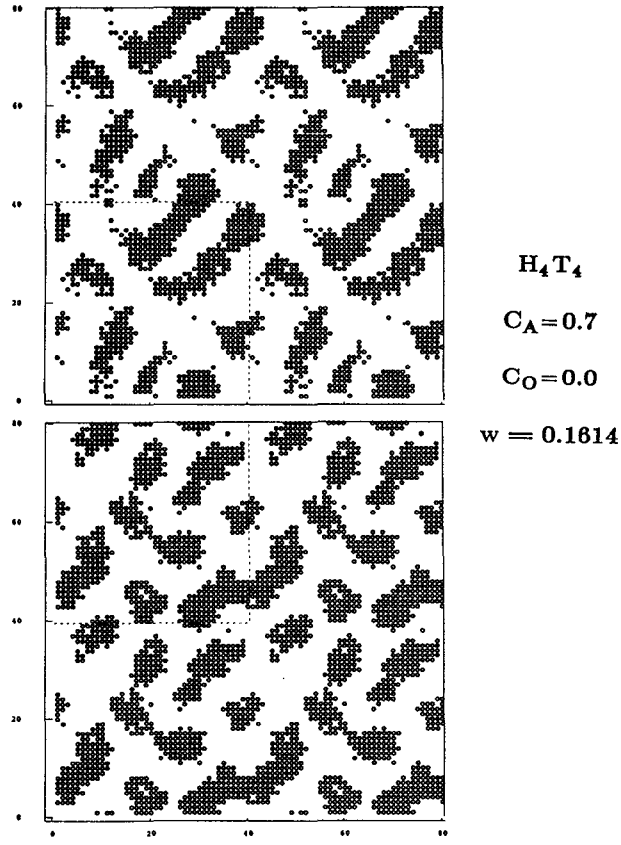

FIG. 11. Two mutually perpendicular slices of $40\times40\times40$ lattice containing 70% H_4T_4 in water at $w = 0.1614$.

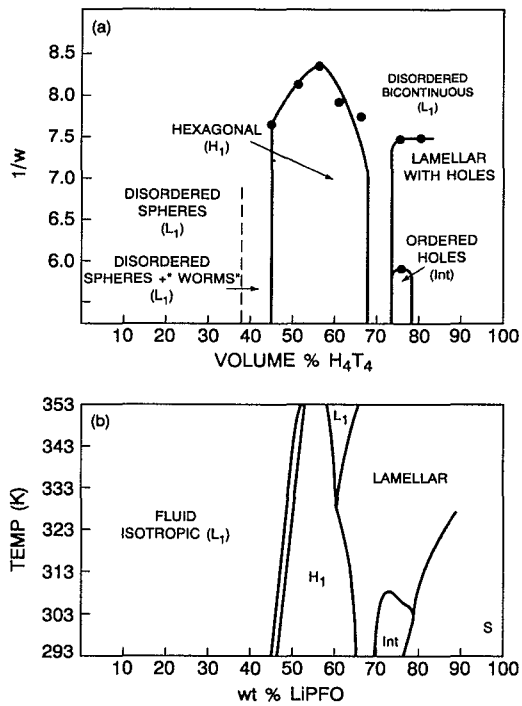

FIG. 12. (a) Approximate phase diagram for H_4T_4 in water determined by Monte Carlo simulation; (b) phase diagram for lithium perfluorooctanoate in water determined by Kekicheff and Tiddy (Ref. 7).

der into lamellar phases with holes. *A priori*, one might expect the phase diagram for our model H_4T_4 surfactant to be most akin to those for nonionic surfactants than to that for the ionic surfactant lithium perfluorooctanoate. However, nonionic surfactants in water typically form cubic intermediate phases rather than birefringent intermediate phases,[7,59] and we have found lamellae with holes, but no cubic phases for solutions containing H_4T_4, H_3T_3, H_5T_5, and H_4T_8. We note that recent neutron scattering studies have shown the existence of intermediate phases in the diblock copolymer poly(ethylenepropylene)-poly(ethylethylene); these phases probably consist of ordered lamellar holes,[14] and are hence analogous to birefringent intermediate phases of surfactant systems. Thus a subtle balance of factors evidently controls the selection of the preferred intermediate phase. Our Monte Carlo simulations should be able to shed some light on this balance, since in the simulations both surfactant architecture and interaction parameters can be precisely controlled.

B. Micellization: Geometric and topological transitions

We now consider the sizes, shapes, and topologies of structures that form in disordered phases at lower concentrations of amphiphile in water. The first problem is to determine the conditions required to obtain micelles. Figure 13 is a semi-log plot of the volume fraction of amphiphile residing, on average, in aggregates of a given size for the amphiphile H_2T_2 at the temperature $w = 0.1538$. Here, an amphiphile molecule belongs to an "aggregate" if any unit in the tail of that amphiphile is adjacent to the tail of any other member of the aggregate. An "adjacent" unit is one of the 26 nearest or diagonally nearest neighbors. To obtain the size distribution plotted in Fig. 13, a system with a given concentration of amphiphile is first cooled slowly to $w = 0.1538$ in small increments of w to maintain thermodynamic equilibrium, just as was done with the systems discussed already. Then the numbers of aggregates of all sizes are counted. The run is then continued for a few hundred thousand more MC steps to allow aggregates to exchange amphiphiles so that a different sample of the size distribution is obtained, and the numbers of aggregates of each size are again counted. This procedure is repeated 1000 or more times, so that at least 1000 "snapshots" of the distribution of aggregates can be obtained. Averaging together the results of these 1000 or more "snapshots," a fairly continuous distribution of at least the smaller aggregate sizes is obtained. To reduce further the statistical fluctuations present in the less common larger aggregates, we then smooth the distribution for aggregates larger than ten molecules in size by averaging together p-mers, where p ranges from $n-2$ to $n+2$, and assign this average to the inventory for n-mers. This additional averaging (for n greater than 10) reduces the fluctuations, but otherwise has little effect on the distribution.

Note in Fig. 13 that for H_2T_2, the volume fraction of n-mers is a monotonically decreasing function of n, although the rate of decrease with n is lessened when the amphiphile concentration is increased. In contrast, in Fig. 13 for H_3T_3, the volume fraction of n-mers monotonically decreases with n only when the amphiphile concentration C_A is 3% or less; when C_A is 4% or greater, a hump appears, centered at an aggregation number of about 60. This hump, of course, represents *micelles* with a fairly broad size distribution, and a critical micelle concentration (CMC) of about 3%. The critical micelle concentration can be estimated not only from the concentration required to form a hump in the distribution function, but also from the concentration of isolated amphiphiles (i.e., 1-mers) when this concentration is high enough to form micelles. Note from Fig. 14 that the concentration of isolated amphiphiles and of pre-micelles ($n < 20$) is roughly independent of total amphiphile concentration, once the CMC is exceeded.

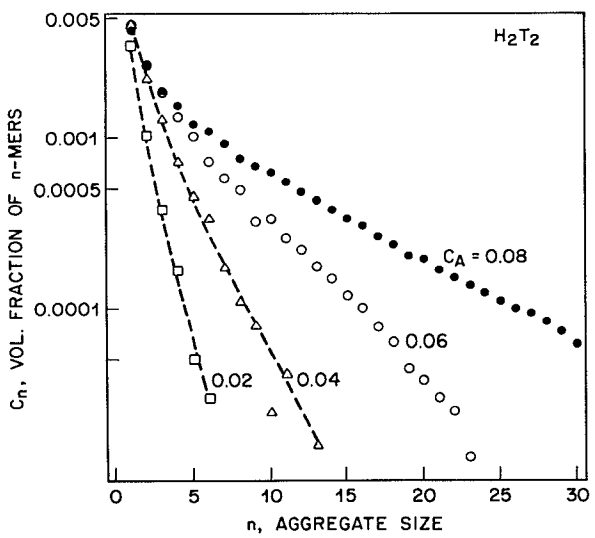

FIG. 13. Volume fraction of amphiphile H_2T_2 in aggregates with aggregation number n for different total amphiphile volume fractions C_A.

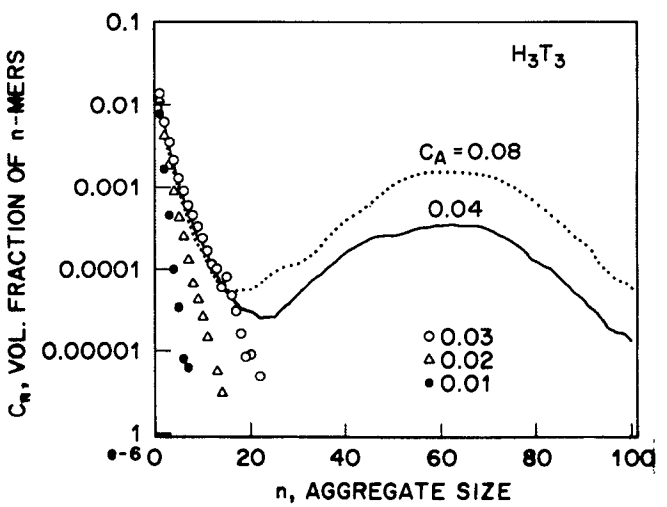

FIG. 14. Volume fraction of surfactant H_3T_3 in aggregates with aggregation number n for different total surfactant volume fractions C_A.

The amphiphile H_2T_2, at least at $w = 0.1538$, is too small to produce micelles. It is also too small to produce, at higher concentrations, any liquid crystalline phases for $w \leqslant 0.1538$ (80% H_2T_2 in 10% oil and 10% water does, however, form a lamellar crystal when cooled to $w = 0.2154$). H_2T_2 should therefore not be regarded as a surfactant, but as a mere amphiphile, analogous to small alcohols such as butanol. H_3T_3, on the other hand, is capable of micellizing, and forming lamellar phases at $w = 0.1538$, as we have seen. It can also form irregular bicontinuous phases, and quasihexagonal arrays of cylinders. It should thus be considered a surfactant. The amphiphile H_1T_3 in water does not form micelles at $w = 0.1538$. Instead, it precipitates out of water into a phase containing mostly H_1T_3; the short heads are mixed with the tails in this phase. If, however, the heads are made to repel each other, rather than interacting the same way that heads interact with water,[59] we expect that H_1T_3 will form micelles. For nonrepelling heads, however, the smallest micelle-forming amphiphile at $w = 0.1538$ has at least two head units and at least three tail units.

Let us now consider an amphiphile that is larger than the minimum required for micelle formation, namely H_4T_4. Figure 15 is a *linear* plot of the distribution of aggregate sizes obtained for H_4T_4 at $C_A = 8\%$, 12%, and 20%. It can be seen from Fig. 15 that the concentration of isolated amphiphiles is about 0.3%; from what was said earlier, this is roughly the value of the CMC. This low value of the singlet surfactant concentration greatly impedes the rate of exchange of surfactant among the aggregates. As the surfactant concentration is reduced towards the CMC, the number of micelles decreases, and an excessive number of Monte Carlo steps are required to get good statistics for the aggregate size distribution. Even at 12% surfactant, 8×10^9 MC steps are required to obtain good statistics; and at 8% surfactant, 16×10^9 steps are required. Furthermore, the micelles that form are large and, thus, an appreciable volume fraction of surfactant is required to form even a few micelles. On a $40 \times 40 \times 40$ lattice, a single micelle of typical aggregation number (about 80) occupies 1% of the lattice volume! Thus, unless C_A is at least a few percent, there is not enough surfactant on the lattice to form micelles whose distribution of sizes is typical of equilibrium. Instead, fractions of micelles form, and these are artifacts of the limited size of the lattice. Thus, to obtain an acceptable micelle size distribution, the total amount of surfactant needs to be several times larger than the amount required to form a single micelle and, hence, well above the CMC. The number-averaged aggregation number $\bar{n}$ and standard deviation σ of aggregates larger than $n = 10$ for H_3T_3 and H_4T_4 are tabulated in Table V.

Note from Fig. 15 that for H_4T_4 at $C_A = 0.20$, a second small peak appears at an aggregation number roughly double that of the main peak. These larger micelles are made still larger, and the proportionate number of them is increased, by increasing the concentration of surfactant, by lowering the temperature, or by making the head of the surfactant shorter than the tail. The last two of these effects are illustrated in Fig. 16, which shows the micelle size distribution for 12% H_3T_4 at the two temperatures $w = 0.1231$ and $w = 0.1538$. This figure shows that for this surfactant, as the temperature is lowered from $w = 0.1231$ to 0.1538, a new peak appears at an aggregation number of around 370. Inspection of the system at this temperature reveals that these are *cigar-shaped* micelles with a diameter similar to that of the spherical micelles that coexist with them. The spherical micelles become larger as the temperature is lowered; this is shown by the shift of the main peak from an aggregation number of about 65 to about 105. In addition, the concentration of pre-micelles, i.e., aggregates with sizes in the range 10–50 or so, virtually vanishes when the temperature is lowered to $w = 0.1538$, and the CMC, estimated from the concentration of singlets, decreases from about 0.8% to 0.2%.

Elongated micelles can also be produced by an increase in surfactant concentration. A 20% concentration of H_4T_4 produces mostly spherical micelles at $w = 0.1538$ (see Fig. 15). When the concentration is increased to 40%, both elongated and spherical micelles appear, with roughly half of the surfactant residing in oblong micelles, and the rest in spheri-

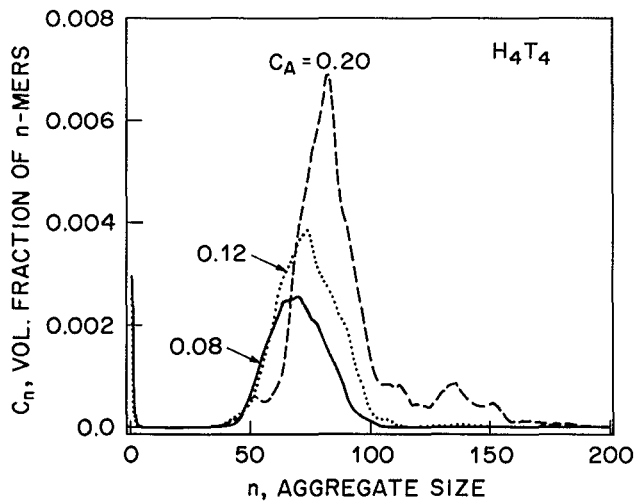

FIG. 15. Volume fraction of surfactant H_4T_4 in aggregates with aggregation number n for different total surfactant volume fractions C_A. Unlike Figs. 13 and 14, the data are here plotted on a linear scale.

TABLE V. Average size and polydispersity of micelles.

	C_A	$\bar{n}$	σ
H_3T_3	4%	43.4	16.2
H_3T_3	6%	51.5	15.2
H_3T_3	8%	61.5	22.8
H_4T_4	8%	68.3	11.7
H_4T_4	12%	72.4	13.1
H_4T_4	20%	84.1	20.8

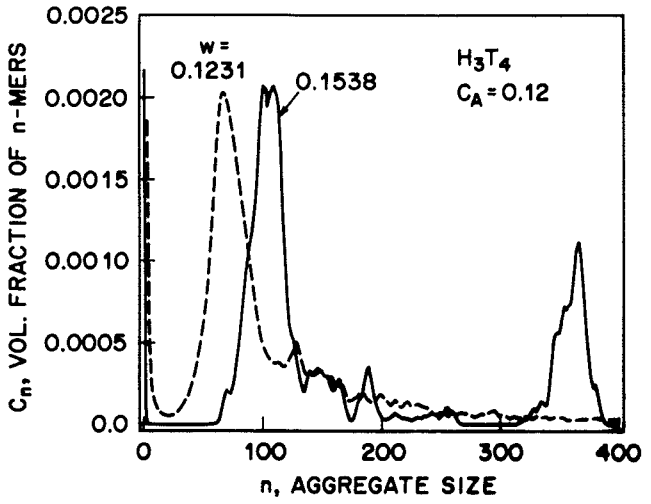

FIG. 16. Volume fraction of surfactant H_3T_4 in aggregates with aggregation number n for $C_A = 0.12$ at $w = 0.1231$ and 0.1538.

cal micelles. The oblong micelles again have diameters comparable to the spherical micelles and they range in length from cigars with an aspect ratio of three or four to worms that are roughly ten times as long as they are wide. The "worms" are not straight, but have an apparent persistence length that is roughly equal to their length. Wormlike micelles have been reported in the experimental literature for both surfactants[60–62] and block copolymers.[57] It is not too surprising that a transition from all spherical to a mix of spherical and cylindrical micelles occurs as the concentration of H_4T_4 is increased to 40%, since at 45% H_4T_4 the system forms infinitely long cylinders (in a hexagonal array).

Thus, our simulations are consistent with free-energy calculations that account for packing constraints and optimal micelle surface area per head group; these show that ellipsoidal micelles are not favored because they require the surface area per head group to deviate from the preferred value almost everywhere on the micelle surface.[63] Thus, as some parameters such as concentration changes, spherical micelles are not likely to grow continuously through ellipsoidal and then to cylindrical shapes. Instead, our simulations show the formation of a bimodal distribution, with spherical micelles coexisting with cigarlike or wormlike ones; this finding agrees with microscopy studies of surfactant and block copolymer systems.[57]

Studies with H_3T_4 show that even a small asymmetry in the relative lengths of the head and tail units can have a significant effect on the geometry of the aggregates that form. When the tail is a little longer than the head, some oblong or cylindrical micelles tend to form, along with spherical micelles, at low surfactant concentrations. If the tail is much longer than the head, then only oblong micelles form, even at low surfactant concentration. At concentrations as low as 10%, these micelles tend to intersect each *other*, if the head is as small as only two units. We have observed intersecting cylindrical or wormlike micelles in both 10% H_2T_4 and in 20% H_2T_6 at $w = 0.1538$. Apparently in these cases the energetic cost of an intersection of two long micelles is not high enough to overcome the entropy cost for these micelles to avoid each other. Figure 17 shows a three-dimensional image of 20% H_2T_2 in water. This image appears to be a network of intersecting cylindrical micelles, and hence is bicontinuous. Disordered bicontinuous phases also form when H_2T_6 is dissolved in water at concentrations higher than 20%, but with 40% H_2T_6 in water, a "sheet network" forms which is distinctly different from the "cylinder network" for 20% surfactant.

IV. CONCLUDING REMARKS

We have found that the ordering transition temperature for a symmetric surfactant in equal amounts of oil and water decreases with decreasing surfactant concentration. At a high surfactant concentration, this ordering transition is strongly first order, while at lower surfactant concentration, the transition is much more continuous. In both cases, the surfactant molecules stretch, i.e., they increase their end-to-end separation, as the transition is approached. At high concentration of surfactant, the strength of the transition and the transition temperature are qualitatively consistent with what one would predict by extrapolating the Fredrickson–Helfand theory for long block copolymers to small amphiphiles. At lower surfactant concentration, the weakness of

FIG. 17. Three-dimensional image of a $40 \times 40 \times 40$ system containing 20% H_2T_6 in water at $w = 0.1538$. This image has been periodically replicated, so that two copies of the same structure are present.

the transition and its two-stage character, seem to be consistent with the predictions of some film models; however, the stretching of the surfactant chain is not consistent with some of the simpler film models. Much more detailed comparisons of the predictions of our Flory-type lattice model with the predictions of film models should soon be possible.

In water only, there are strongly first-order transitions to lamellar and hexagonal phases at compositions similar to those at which these transitions occur in block copolymer systems and in some surfactant systems. As the concentration of surfactant in water is reduced from that at which lamellae form toward that required for cylinders, holes rapidly multiply in the layers containing tails. If the holes are plentiful enough, hexagonal ordering of the holes within each layer occurs when the temperature is lowered. A similar ordering of holes has been observed in some surfactant and block copolymer systems.

We find in our simulations a minimum amphiphile length for micelle formation; and the CMC is very sensitive to surfactant length. The micelle shape is sensitive to head/tail asymmetry in the surfactant; spherical and wormlike micelles can coexist, and ellipsoidal micelles are not favored. Various kinds of disordered bicontinuous phases can form, depending on surfactant concentration, surfactant architecture, and the oil/water concentration ratio.

The consistency of these findings with known results is a heartening indicator that our simple model has no major defects that would disqualify it from describing the qualitative behavior of real surfactant systems. Hence, in the future the model can be used with some confidence to attempt to increase our understanding of surfactant solutions. As computing power continues to increase, issues that can be addressed with the simulation technique include the following: the structural differences among the various types of *disordered* bicontinuous phases and how these types depend on composition and surfactant architecture; the dependence on surfactant architecture of the types of *ordered* bicontinuous phases that might form; the validity and limitations of film models as well as calculations of the film bending constants in those models; verification of the two-stage nature of the ordering transition for symmetric surfactants at low concentrations at an oil/water ratio of unity; the sizes, shapes, and surfactant partitioning in micelles containing two different surfactants; and the effect of head–head repulsion on surfactant phase behavior.

ACKNOWLEDGMENT

I am grateful to Karen Winey for her critical review of an earlier version of this manuscript.

[1] *Processing, Structure, and Properties of Block Copolymers*, edited by M. J. Folkes (Elsevier, New York, 1985).
[2] *Developments in Block Copolymers -1*, edited by I. Goodman (Applied Science Publishers, New York, 1982).
[3] H. T. Davis, J. F. Bodet, L. E. Scriven, and W. G. Miller, in *Physics of Amphiphilic Layers*, edited by J. Meunier, D. Langevin, and N. Boccara (Springer-Verlag, New York, 1987).
[4] E. L. Thomas, D. J. Kinning, D. B. Alward, and C. S. Henkee, Macromolecules **20**, 2934 (1987).
[5] Y. Shen, C. R. Safinya, L. Fetters, M. Adam, T. Witten, and N. Hadjichristidis, Phys. Rev. A **43**, 1886 (1991).
[6] P. Kekicheff and B. Cabane, J. Phys. (Paris) **48**, 1571 (1987).
[7] P. Kekicheff and G. J. T. Tiddy, J. Phys. Chem. **93**, 2520 (1989).
[8] E. L. Thomas, D. B. Alward, D. J. Kinning, D. C. Martin, D. L. Handlin, Jr., and L. J. Fetters, Macromolecules **19**, 2197 (1986).
[9] V. Luzzati and P. A. Spegt, Nature **215**, 701 (1967).
[10] A. Tardieu, thesis, Universite Paris-Sud Orsay, 1972.
[11] W. Helfrich, in *Physics of Defects*, 1980 Les Houches, Session XXXV, edited by R. Balian *et al.* (North-Holland, Amsterdam, 1981).
[12] W. Helfrich, J. Phys. (Paris) **48**, 291 (1987).
[13] J. Charvolin and J. F. Sadoc, J. Phys. (Paris) **48**, 1559 (1987).
[14] K. Almdal, K. A. Koppi, F. S. Bates, and K. Mortensen, Macromolecules **25**, 1743 (1992).
[15] S. T. Hyde, S. Andersson, B. Ericsson, and K. Larsson, Z. Kristallogr. **168**, 213 (1984).
[16] L. E. Scriven, in *Micellization, Solubilization, and Microemulsions*, edited by K. L. Mittal (Plenum, New York, 1977).
[17] W. Jahn and R. Strey, J. Phys. Chem. **92**, 2294 (1988).
[18] M. Kahlweit, Science **240**, 617 (1988).
[19] L. Auvray, J.-P. Cotton, R. Ober, and C. Taupin, in *Physics of Complex and Supermolecular Fluids*, edited by S. A. Safran and N. A. Clark (Wiley–Interscience, New York, 1987).
[20] S. M. Gruner, J. Phys. Chem. **93**, 7562 (1989).
[21] C. D. Turner, PhD. thesis, Princeton University, 1990.
[22] H. Hasegawa, K. Tanaka, K. Yamasaki, and T. Hashimoto, Macromolecules **20**, 1651 (1987).
[23] Y. Talmon and S. Prager, J. Chem. Phys. **69**, 2984 (1978).
[24] P. G. de Gennes and C. Taupin, J. Phys. Chem. **86**, 2294 (1982).
[25] B. Widom, J. Chem. Phys. **81**, 1030 (1984).
[26] D. Andelman, M. E. Cates, D. Roux, and S. A. Safran, J. Chem. Phys. **87**, 7229 (1987).
[27] L. Golubovic' and T. C. Lubensky, Phys. Rev. A **41**, 4343 (1990).
[28] D. Andelman, M. E. Cates, D. Roux, and S. A. Safran, J. Chem. Phys. **87**, 7229 (1987).
[29] D. A. Huse and S. Leibler, J. Phys. (Paris) **49**, 605 (1988).
[30] M. E. Cates, D. Andelman, S. A. Safran, and D. Roux, Langmuir **4**, 802 (1988).
[31] L. Leibler, Makromol. Chem. Macromol. Symp. **16**, 1 (1988).
[32] Z. G. Wang and S. A. Safran, J. Phys. (Paris) **51**, 185 (1990).
[33] M. E. Cates, D. Roux, D. Andelman, S. T. Milner, and S. A. Safran, Europhys. Lett. **5**, 733 (1988).
[34] S. A. Safran, P. Pincus, and D. Andelman, Science **248**, 354 (1990).
[35] S. A. Safran, J. Chem. Phys. **78**, 2073 (1983).
[36] S. A. Safran, P. A. Pincus, D. Andelman, and F. C. Mackintosh, Phys. Rev. A **43**, 1071 (1991).
[37] I. Szleifer, D. Kramer, A. Ben-Shaul, D. Roux, and W. M. Gelbart, Phys. Rev. Lett. **60**, 1966 (1988).
[38] E. Helfand, Macromolecules **8**, 552 (1975); E. Helfand and Z. R. Wasserman, *ibid.* **9**, 879 (1976).
[39] L. Leibler, Macromolecules **13**, 1602 (1980).
[40] G. H. Fredrickson and E. Helfand, J. Chem. Phys. **87**, 697 (1987).
[41] M. Olvera de la Cruz, Phys. Rev. Lett. **67**, 85 (1991).
[42] B. Owenson and L. Pratt, J. Phys. Chem. **88**, 2905 (1984).
[43] J. M. Haile and J. P. O'Connell, J. Phys. Chem. **88**, 6363 (1984).
[44] K. Watanabe, M. Ferrario, and M. L. Klein, J. Phys. Chem. **92**, 819 (1988).
[45] B. Smit, P. A. J. Hilbers, K. Esselink, L. A. M. Rupert, N. M. van Os, and A. G. Schlijper, Nature **348**, 624 (1990); J. Phys. Chem. **95**, 6361 (1991).
[46] B. Widom, J. Chem. Phys. **84**, 6943 (1986).
[47] M. Schick and W. H. Shih, Phys. Rev. B **34**, 1797 (1986); M. Gompper and M. Schick, Phys. Rev. Lett. **62**, 1647 (1989).
[48] R. G. Larson, J. Chem. Phys. **89**, 1642 (1988).
[49] R. G. Larson, J. Chem. Phys. **91**, 2479 (1989).
[50] R. G. Larson (unpublished).
[51] S. Okamoto, H. Hasegawa, T. Hashimoto, L. Fetters, D. Gobran, Z. Xu, and E. L. Thomas (unpublished).
[52] B. Minchau, B. Dünweg, and K. Binder, Polym. Comm. **31**, 348 (1990).
[53] G. Hadziioannou and A. Skoulios, Macromolecules **15**, 258 (1982).
[54] K. Almdal, J. H. Rosedale, F. S. Bates, G. D. Wignall, and G. H. Fredrickson, Phys. Rev. Lett. **65**, 1112 (1990).
[55] J.-L. Barrat and G. H. Fredrickson, J. Chem. Phys. **95**, 1281 (1991).
[56] D. J. Kiney, K. I. Winey, and E. L. Thomas, Macromolecules **21**, 3502 (1988); K. Winey, E. L. Thomas, and L. Fetters, *ibid.* (to be published).
[57] K. Winey, PhD. thesis, Univ. of Mass., 1991.

[58] J. D. Ferry, *Viscoelastic Properties of Polymers*, 3rd ed. (Wiley, New York, 1980).
[59] R. G. Larson, PhD. thesis, University of Minnesota, 1980.
[60] S. Kumar, L. Yu, and J. D. Litster, Phys. Rev. Lett. **50**, 1672 (1983).
[61] P. J. Missel, N. A. Mazer, G. B. Benedek, C. Y. Young, and M. C. Carey, J. Phys. Chem. **84**, 1044 (1980).
[62] S. A. Safran, L. A. Turkevich, and P. Pincus, J. Phys. (Paris) Lett. **45**, L 69 (1984).
[63] J. N. Israelachvili, D. J. Mitchell, and B. W. Ninham, J. Chem. Soc., Faraday Trans. **72**, 1525 (1976).